

# Improvement in Geometrical Resolution of Plastic Laser Sintering by using Reduced Spot Sized Laser

Toshiki NIINO and Keisuke MORITA

Institute of Industrial Science, the University of Tokyo, Japan

4-6-1 Komaba Meguro Tokyo, 153-8505 Japan

niino@iis.u-tokyo.ac.jp

**ABSTRACT** Reviewed, accepted September 23, 2010

Plastic laser sintering is one of the most promising processes for rapid manufacturing among various additive manufacturing (AM) technologies. Though the process tends to be applied to fabrication of larger parts in comparison to stereolithography, its ability of creating complex structure as an advantage of additive manufacturing technologies should be demonstrated in production of smaller parts and parts including fine and complex geometries as well. In this research, narrow CO<sub>2</sub> laser beams with spot diameters of 130μm and 150μm were tested while the commercially available machines are equipped with those around 500μm. Relationship between resolution (available wall thickness) and spot diameter is proportional when the diameter is greater than 150μm, but effect of reducing the spot size further is not significant. The minimum wall thickness of 180μm was obtained, but this part was so fragile that skill in breakout treatment is critical. To discuss the mechanical strength of micro-plastic-laser-sintering, packing rate of obtained parts was introduced as an index of the strength. Build parameter that minimizes the wall thickness without decreasing the tensile strength below 30MPa was searched, and a set of parameters that provides minimal thickness of 0.6mm was obtained. Reducing laser spot size inevitably leads to shrinkage of scanning range of galvanometer mirrors. To overcome this problem, the whole laser scanning system was set on an X-Y positioner which are driven by stepper motors. The whole exposure area is divided into some regions each of which is smaller than range of galvanometer mirror system, and it is exposed by repeating fast scanning by galvanometer mirrors and slow sliding by the X-Y positioner. Problems occurring at the region boundary were investigated. As counter measures, overlapping of exposure areas and switching of region boundary are introduced and successfully eliminate the problem.

## NOMENCLATURE

$m_s$ : mass of a sinter  
 $t_m$ : Melting temperature

$t_n$ :	Nominal wall thickness
$v_b$ :	Bulk volume of powder or a sinter
$\beta$ :	Packing rate of powder or a sinter
$\rho_t$ :	True density of powder material

## INTRODUCTION

Plastic laser sintering is one of the most promising rapid manufacturing methods among various additive manufacturing technologies that have ever been developed and commercialized. A wide choice of applicable thermoplastics facilitates fabrication of functional parts or devices with various material performances such as heat resistance, mechanical strength and biodegradability[1]. On the other hand, in terms of geometrical preciseness of fabricated parts, the process is inferior to some other additive manufacturing processes such as stereolithography. Because of this disadvantage, selective laser sintering tends to be used for fabrication of larger parts. Thus, the most rapid manufacturing examples that have ever been developed are relatively large and including simple structures. However, additive manufacturing is more cost effective when smaller parts are fabricated[2] since the cost is roughly proportional to process time or volume of each part. Additionally, fabrication of more complex structure in smaller dimensions can give a better chance to demonstrate advantage of additive manufacturing over the other conventional processes.

The leading cause of the poor preciseness of plastic laser sintering is large laser beam diameter in commercially available systems. In a typical plastic laser sintering system, CO<sub>2</sub> laser, whose wavelength is 10.6 $\mu$ m, is focused into a spot of 500 $\mu$ m in diameter while a typical stereolithography system employs near UV laser whose wavelength is around 350nm and focuses into a small diameter of 50 $\mu$ m or smaller. Due to its longer wave length, to focus CO<sub>2</sub> laser into a small spot is more difficult than UV laser, but there is still some room to reduce the diameter from theoretical point of view, and, in reality, we find a small focal spot less than 100 $\mu$ m in some CO<sub>2</sub> laser applications such as laser drilling. In this research, the effect of reducing laser spot diameter on improvement in preciseness of the plastic laser sintering as a process of machining is investigated. Two experimental setups equipped with optical systems that can focus their lasers into small spots of 130 $\mu$ m and 150 $\mu$ m, respectively, were built and tested. Relationship between thickness of vertical wall and various process parameters are examined. Packing rate of the walls are measured as an index for their mechanical strength. MicroCT observation was performed to investigate distribution of pores in the thin walls.

As mentioned previously, reducing spot diameter of CO<sub>2</sub> laser to less than 100μm is not very difficult from the theoretical view point. However, it is not reasonable from the side of practice since it makes a sacrifice of scanning range of galvanometer mirrors resulting in the shrinkage of the build envelope. To overcome this drawback, a hybrid system consisting of galvanometers and stepper motors was tested (Fig. 1). In this system, the whole galvanometer mirror system including focusing optics is set on an X-Y positioner that is driven by the stepper motors. The stepper motors cannot scan the laser spot as fast as the galvanometers but can provide greater range of movement more easily and economically. Utilizing this advantage, we can expand the build envelope in scan and stitch way; we divide the whole exposure area into small regions, expose one of them by high speed scanning with galvanometer mirrors, and convey the galvanometer mirror system with the X-Y positioner to expose another region. Since moving the galvanometer system to the next region takes time, there is a time lag between exposures of two neighboring regions. This difference may cause problems when a cross section which lays across a region boundary. This paper reveals the problem and introduces its counter measure.

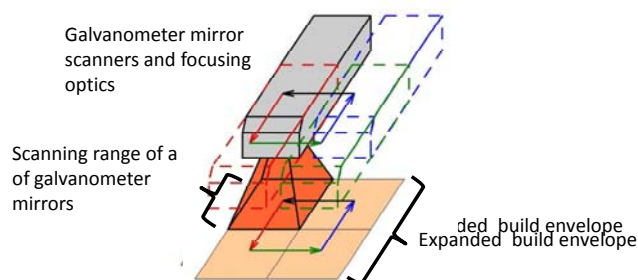


Fig. 1 Schematic view for build envelope expansion by scan-and-stitch

## LASER OPTICS AND POWDER

In this research, two sets of laser optics were used. One is a commercially available laser marker (ML-G9320, KEYENCE). This device, “scanner A” in the following description, is equipped with CO<sub>2</sub> laser, and its beam is focused on the powder surface in a diameter of 150μm. Distance between lens and the focal plane is 113mm, and scanning range is 55mm x 55mm.

The other one, “scanner B” in the following description, was designed specially for our purpose. This optics is also installed with CO<sub>2</sub> laser. The beam emitted from the laser tube is once expanded to 17mm in diameter, then bent by galvanometer mirrors up to 19° at the maximum and focused on the powder surface by a lens with focal length of

Tbl. I Parameters of scanners

Laser scanner	A	B
Wave length ( $\mu\text{m}$ )	10.6	
Laser mode	Single mode	
Spot diameter ( $\mu\text{m}$ )	150	130
Work distance (mm)	113	109
Exposure range (mm)	55 x 55	100x100
Scanning resolution ( $\mu\text{m}$ )	1	1

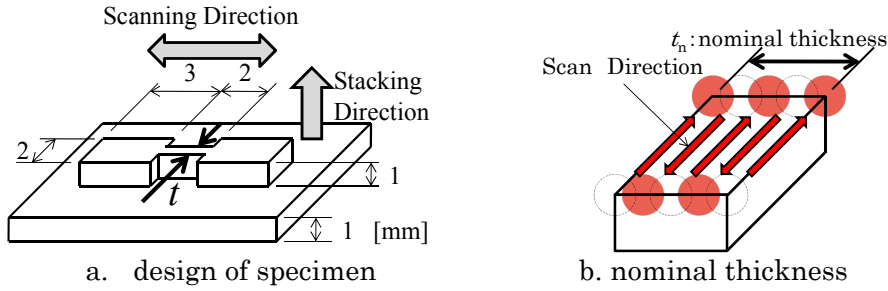


Fig. 2 Measurement of wall thickness measurement

Tbl. II Building condition of thin vertical wall test

Laser power	4.0W
Scanning velocity	3.8m/s
Scanning interval	80 $\mu\text{m}$
Layer thickness	100 $\mu\text{m}$
Powder bed temperature	$t_m-3\text{K}$

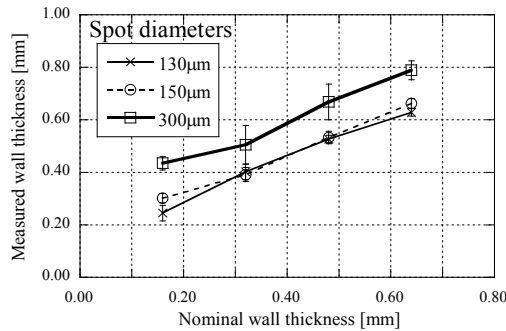


Fig. 3 Relationships between measured thickness and nominal thickness

109mm. By this optic system, a  $1/e^2$  diameter of 130 $\mu\text{m}$  is obtained. Parameters of laser optics employed in this research are summarized in Tbl. I.

As the powder, ASPEX-PA produced by ASPECT Inc. was employed in the experiments of this research. This powder is PA12 and has the average grain size of 45 $\mu\text{m}$ .

## FABRICATION OF FINE STRUCTURE BY REDUCED LASER SPOT

### RELATIONSHIP BETWEEN WALL THICKNESS AND SPOT DIAMETER

Minimum thickness of thin vertical wall can be good index of machining precision. A design depicted by Fig. 2a was used as that for the test specimen employed in this research and the thickness at the center of the wall, which is denominated by “ $t$ ,” was

measured. Laser is scanned in the longitudinal direction of the wall, and we define the distance between the central lines of the outmost scans as the nominal thickness of the wall,  $t_n$  (Fig. 2b). Building condition as displayed in Tbl. II is employed for the specimen preparation.

Relationships between measured thickness and nominal thickness when various spot diameters were used are shown in Fig. 3. The spot diameter of 300 $\mu\text{m}$  was obtained by defocusing the optics of scanner B. Though reducing spot diameter from 300 $\mu\text{m}$  to 130 $\mu\text{m}$  or 150 $\mu\text{m}$  improved fineness quite clearly, difference between 130 $\mu\text{m}$  and 150 $\mu\text{m}$  is negligible.

Though all build parameters except nominal thickness and spot size were the same in the previous experiments, they should be modified according to the spot size. In the following experiments, each parameters except layer thickness is adjusted so that its nominalization by spot size is equalized. With respect to the spot sizes of 150 $\mu\text{m}$  and 300 $\mu\text{m}$ , wall thickness measurements were performed using build parameters as shown in Tbl. III. The same layer thickness was used for the both spot diameters because reducing the layer thickness from the current value of 100 $\mu\text{m}$  is difficult or impossible due to difficulty of coating thin layer. As depicted in Fig. 4, relationships between actual and nominal wall thicknesses in normalized form for two diameters are in very good accordance.

Tbl. III Build parameters of which normalization by spot diameter are equalized

Spot diameter	150 $\mu\text{m}$	300 $\mu\text{m}$
Scan speed	2.0m/s	4.0m/s
Scan spacing	50 $\mu\text{m}$	100 $\mu\text{m}$
Layer	100 $\mu\text{m}$	100 $\mu\text{m}$
Laser power	1.2W	4.8W
Part bed temp.	$t_m-4\text{K}$	$t_m-4\text{K}$

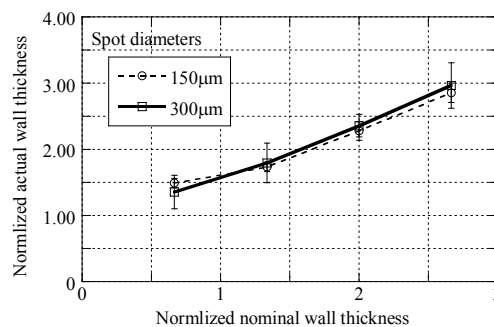


Fig. 4 Relationships between normalized measured thickness and normalized nominal thickness

### PARAMETER OPTIMIZATION FOR THICKNESS MINIMIZATION

By optimizing the process parameters to minimize the wall thickness (Tbl. IV), a wall as thin as 180 $\mu\text{m}$  was obtained. The wall was so fragile that even removing unsintered powder around the part can easily destroy it. In other words, the minimum wall thickness is dependent on the level of skills in powder removal (breakout process) as well as build parameters such as laser power. However, standardizing the breakout process to remove unsintered powder necessarily and sufficiently is very difficult. Moreover, building such a weak part does not make sense. We will discuss the strength of the thin wall in the following section.

Tbl. IV Build parameter for the thin wall with the minimal thickness

Nominal thickness	165 $\mu\text{m}$	Scanning velocity	3.8m/s
Beam diameter	130 $\mu\text{m}$	Layer thickness	100 $\mu\text{m}$
Laser power	0.43W	Powder bed temp	$t_m - 4\text{K}$

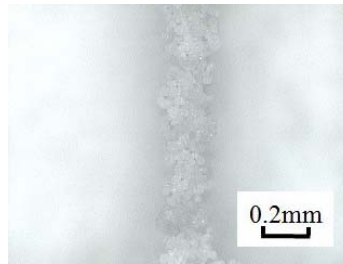


Fig. 5 Vertical wall of 180 $\mu\text{m}$  in thickness

### DENSITY OF THIN WALL

The mechanical strength of a part that is fabricated by an AM technique is dependent on its build parameters while the strength of a part obtained by subtractive processes maintains; subtractive processes preserve the strength, and AM process decides that. Thus, we should discuss relationship between strength of miniature structure (thin wall in this case) and build parameters, but it is challenging or almost impossible to measure the strength of such a small structures. Since strength and density correlate very closely as shown in Fig. 6, we can use the packing rate as an index for the strength and refer this relationship as the need arises.

To examine the packing rate of miniature parts specimens as depicted in Fig. 7 were prepared using build parameters as shown in Tbl. V. Fig. 8 shows relationship between packing rate and nominal width of specimens. Packing rate was calculated by the following equation,

$$\beta = \frac{m_s}{v_s \rho_t} \quad (1)$$

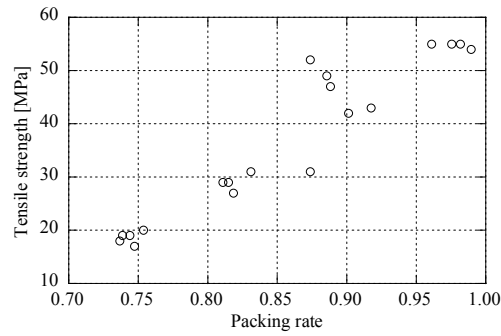


Fig. 6 Relationship between tensile strength and packing rate

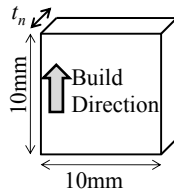


Fig. 7 Test specimen for density measurement

Tbl. V Build parameters of specimen for density measurement

Laser power	1.4W
Scanning velocity	2.0m/s
Scanning interval	40 $\mu$ m
Layer thickness	100 $\mu$ m
Powder bed temperature	$t_m$ -3K

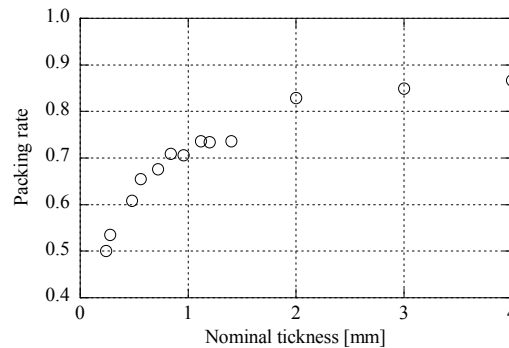


Fig. 8 Relationship between tensile strength and packing density

Here,  $m_s$  and  $v_b$  can be obtained by measuring the specimen. True density of the powder material,  $\rho_t=1.03\text{g/cm}^3$ , which is provided by the powder fabricator. As displayed in Fig. 8, packing rate increases as nominal width is increased. The rate of increase is steep when the width is smaller than 1mm. No specimen with a nominal thickness thinner than 0.16mm was strong enough to stand breakout process.

Packing rate is also affected by supplied laser energy. Fig. 9 shows relationships between packing rate and laser energy supplied to a unit area when nominal widths were set to 0.16mm, 0.48mm and 0.96mm, respectively. The packing rate increased as the supplied energy becomes larger, and it was saturated with the energy is greater than

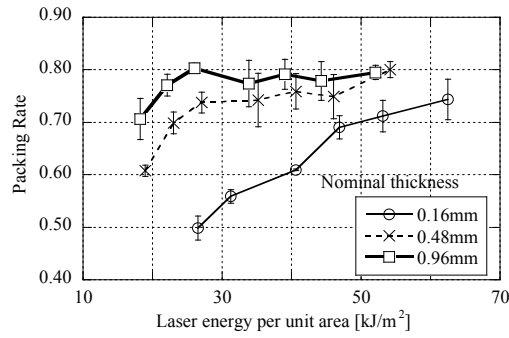


Fig. 9 Relationship between packing rate and supplied laser energy for various nominal thicknesses

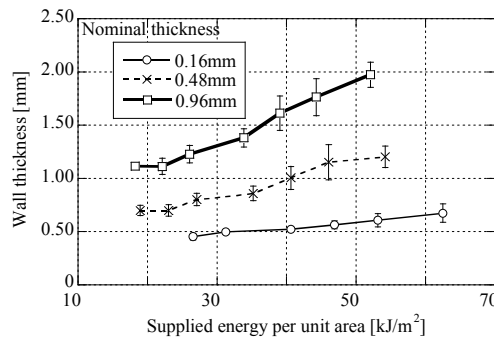


Fig. 10 Relationship between wall thickness and supplied laser energy for various nominal thicknesses

around  $25\text{kJ/m}^2$ , when nominal width was thicker than  $0.48\text{mm}$ . Contrary, saturation was not observed when nominal thickness is  $0.16\text{mm}$ . The actual wall thickness also increased as energy supply is increased (Fig. 10).

Scan interval is also affecting packing rate. Though the scanning interval of  $80\mu\text{m}$  provided the largest packing rate (Fig. 11), the difference from narrower intervals were very small. The difference between  $40\mu\text{m}$  and  $20\mu\text{m}$  is negligible (Fig. 12).

The parameters that can maximize the packing rate with the wall thickness below  $1\text{mm}$  was searched for, and a set of parameters as shown in Tbl. VI was obtained. This set of parameters gave 82% of packing rate with a wall thickness of  $0.95\text{mm}$ .

Fig. 13a is a cross sectional view of this wall, which is obtained by micro CT (SMX-130CT-SV, SHIMADZU) observation. We can find that pores are distributed unevenly, and porosities in the middle and outer portions (Fig. 13b) are 11% and 25%, respectively.

Since packing rate was saturated around 80% in overall tendency, parameters that could minimize the wall thickness with packing rate over 80% was searched, and a set of parameters as shown in was obtained. By referring the relationship between strength and density as shown in Fig. 6, we can estimate the tensile strength of this wall is around  $30\text{MPa}$ , which is equivalent to typical value of stereolithography.

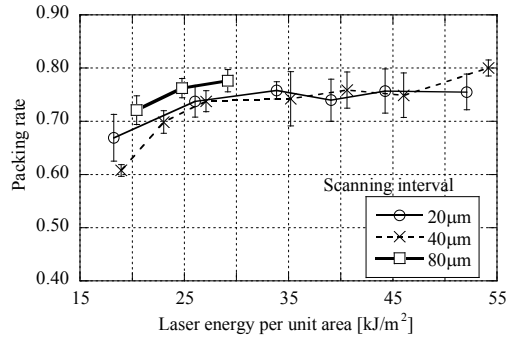


Fig. 11 Relationship between packing rate and laser energy with various scanning intervals ( $t_n=0.48\text{mm}$ )

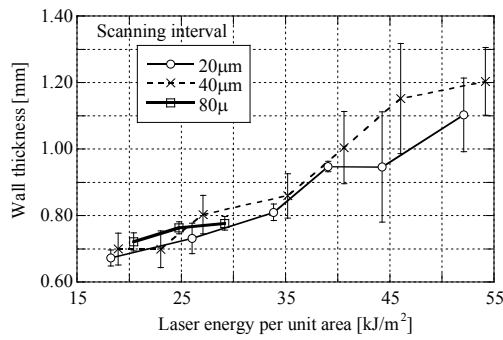
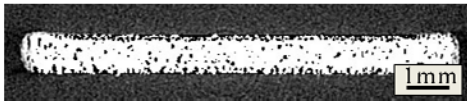


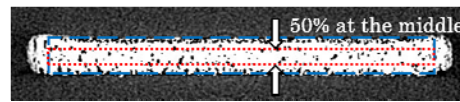
Fig. 12 Relationship between wall thickness and laser energy with various scanning intervals ( $t_n=0.48\text{mm}$ )

Tbl. VI Build parameters for densest wall thinner than 80%

Nominal thickness	0.64mm
Laser power per unit area	28kJ
Scanning interval	80µm
Actual thickness	0.95mm
Packing density	82%



(a) CT reconstruction



(b) porosity measurements

Fig. 13 Micro CT graphs

Tbl. VII Build parameters for thinnest wall denser than 80%

Nominal thickness	0.32mm
Laser power per unit area	31kJ
Scanning interval	60µm
Actual thickness	0.62mm
Packing density	81%

## EXPANSION OF BUILD ENVELOPE

To expand scanning range, a commercially available laser marker (scanner A) was set on X-Y scanner that was driven by a stepper motor and ball-screw system. To examine

the sintering quality at the seam, a specimen as displayed by Fig. 14 was prepared. Since the region that was sintered earlier is cooled while the scanner is conveyed to the next region, insufficient sintering occurs at the seam. As a result, porosity at the seam became 17% while it was 12% at the other place. To compensate this loss of the heat during X-Y scanner operation, exposure for the later region is overlapped on the previously exposed area. Overlapping one scan line could reduce the porosity to 14%, but this is still larger than at non seam cross section. Contrary, overlapping two scan lines results in yellowing. Though there must be optimal parameter of overlapping that can avoid both of oversintering and undersintering, it is not unique since the loss of heat is dependent on various conditions such as geometry of built parts, place of part in building chamber.

In the previous cases, the seaming was performed at the same place in all the layers. This seems to emphasize the effect of undersintering. To disperse the effect, seaming positions were varied by layers. More concretely, two lines are selected as candidates of seams, and seaming position were varied by switching them alternately as depicted by Fig. 15. As a result, the undersintering disappeared and porosity was successfully decreased to 12%.

### DISCUSSIONS

In this research, investigation on fabrication of precise structure with plastic laser sintering is carried out on an experimental basis. Effect of reducing the spot size of laser beam is examined by varying the spot size. Two laser sintering apparatuses were

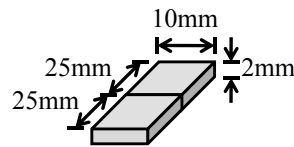


Fig. 14 Specimen for seam quality examination

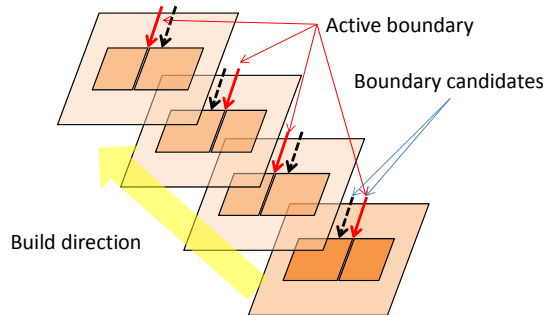


Fig. 15 Dispersion of undersintering effect at the seam

prototyped to use smaller laser spot than commercially available machine can provide. Regenfuss's group took similar way to improve the resolution of laser sintering fabrication of metal and ceramic [3]. They used a very small spot diameter of  $14\mu\text{m}$  [4] and obtained very thin vertical wall of  $40\mu\text{m}$  in thickness with a high aspect ratio of 25. Their device was commercialized already [5]. There are many differences between metal and plastic. First of all, we cannot apply short wavelength laser to plastic laser sintering because of its low absorption to regular plastic while most metal laser sintering or melting devices are using YAG or fiber lasers with short wavelengths around  $1\mu\text{m}$ . Since diffraction limit is proportional to wavelength, focusing laser spot for plastic laser sintering into small spot forces us a sacrifice of scanning range as mentioned in the early section of this paper. Secondly, viscosity of molten plastic is very high and varies very gently with temperature, while a metal melts at its melting point very quickly and viscosity reduces dramatically.

Though this research is carried out on experimental basis, theoretical approach is also very important. With respect to metal sintering or melting, various theoretical models were introduced [6...8] in the early stage of its development. However, behavior of plastic is very much complicated, and recent experiment base report about plastic behavior or characteristic still can provide new and important information [10].

This paper concludes that minimum resolution of plastic laser sintering is around  $0.6\text{mm}$ . It is obvious this resolution is not acceptable as the performance of an RM tool. We have some room for miniaturization of spot size, but large grain size or layer thickness, we guess, is prevent further improvement in resolution of plastic laser sintering. Thus our important challenge is progress in powder handling. In addition, decrease of focal length which is forced by spot size reduction leads to lowering the ceiling of process chamber. This is also troublesome from a practical viewpoint.

## CONCLUSIONS

With respect to minimum thickness of walls, reducing spot diameter to  $150\mu\text{m}$  is quit effective as far as we tested in this research. Since there was no significant difference between  $130\mu\text{m}$  and  $150\mu\text{m}$ , we can guess that precision improvement only by reducing spot size comes to the end. A packing rate of thin part is saturated with about 80%, and this gives tensile strength of  $30\text{MPa}$ . Though this strength is 60% of that for bulky sinter, it is enough strong for some applications. As the minimum wall thickness with this rate,  $0.6\text{mm}$  was obtained. Shrunk exposure range of galvanometer mirror as a drawback of reducing spot size can be overcome completely by introducing build envelope expansion using hybrid system of galvanometer mirrors and stepper motor driven X-Y

positioner.

## REFERENCES

- [1] Niino, T., et al, "SLS Fabrication of Highly Porous Model Including Fine Flow Channel Network Aiming at Regeneration of Highly Metabolic Organs," *Proc. Solid Freeform Fabrication Symposium 2006* (2006) 160-170
- [2] Hopkinson, N., et al, "Rapid Manufacturing," John Wiley & Sons, (2006)
- [3] Exner, H., et al, "Laser micro sintering: A new method to generate metal and ceramic parts of high resolution with sub-micrometer powder," *virtual and physical prototyping*, **3** (2008) 3-11
- [4] Regenfuss, P., et al, "Principles of laser micro sintering," *Rapid Prototyping Journal*, **13** (2007) 204-212
- [5] URL: <http://www.3d-micromac.com/microFORM-en.html> (accessed July 15th 2010)
- [6] Fischer, P., "A model for the interaction of near-infrared laser pulses with metal powders in selective laser sintering," *Appl. Phys. A* **74** (2002) 467-474
- [7] Chen, T., et al, "Numerical simulation of two-dimensional melting and resolidification of a two-component metal powder layer in selective laser sintering process," *Numerical Heat Transfer, A* **46** (2004) 633-649
- [8] Kolossov, S., et al, "3D FE simulation for temperature evolution in the selective laser sintering process," *Int'l J. Machine Tool and Manuf'g*, **44** (2004) 117-123
- [9] Zarringhalam, H., "Degree of particle melt in Nylon-12 selective laser-sintered parts," *Rapid Prototyping Journal*, **15** (2009) 126-132